The Plant Cell, Vol. 8, 1935–1949, November 1996 © 1996 American Society of Plant Physiologists

RESEARCH ARTICLE

Localized Apical Increases of Cytosolic Free Calcium Control Pollen Tube Orientation

Rui Malhó[a,1] and Anthony J. Trewavas[b]

[a] Departamento de Biologia Vegetal, Faculdade de Ciências de Lisboa, R. Ernesto de Vasconcelos, Bloco C2, 1780 Lisboa, Portugal

[b] Molecular Signalling Group, Institute of Cell and Molecular Biology, University of Edinburgh, Rutherford Building, Edinburgh EH9 3JH, United Kingdom

To reach the ovule, pollen tubes must undergo many changes in growth direction. We have shown in previous work that elevation of cytosolic free calcium ($[Ca^{2+}]_c$) can manipulate orientation in growing pollen tubes, but our results suggested that $[Ca^{2+}]_c$ changes either in the tip or in more distal regions might regulate the critical orienting mechanism. To identify the spatial location of the orienting motor, we combined the techniques of ion imaging with confocal microscopy and localized photoactivation of loaded caged Ca^{2+} (nitr-5) and diazo-2 (a caged Ca^{2+} chelator) to manipulate $[Ca^{2+}]_c$ in different pollen tube domains. We found that increasing $[Ca^{2+}]_c$ on one side of the pollen tube apex induced reorientation of the growth axis toward that side. Similarly, a decrease in $[Ca^{2+}]_c$ promoted bending toward the opposite side. These effects could be mimicked by imposing localized external gradients of an ionophore (A23187) or a Ca^{2+} channel blocker ($GdCl_3$); the pollen tubes bend toward the highest concentration of A23187 and away from $GdCl_3$. Manipulation of $[Ca^{2+}]_c$ in regions farther back from the apical zone also induced changes in growth direction, but the new orientation was at random. We observed communication of these distal events to the tip through a slow-moving $[Ca^{2+}]_c$ wave. These data show that localized changes of $[Ca^{2+}]_c$ in the tip, which could result from asymmetric channel activity, control the direction of pollen tube growth.

INTRODUCTION

It is the function of the pollen tube to deliver the sperm cells to the ovary and thus initiate the crucial process of seed development. For successful fertilization, pollen must germinate on the stigma, grow through the style, and find and penetrate the ovule micropyle. These processes require the growing pollen tube to undergo numerous changes in growth orientation. The cues in the stigma that signal pollen tube orientation are believed to be electrical (Malhó et al., 1992), mechanical, and chemical (Heslop-Harrison, 1987; Cheung et al., 1995), but their nature is not well understood.

Pollen tube growth is limited to the tip and is highly polarized. In recent years, substantive progress has been made toward understanding tip growth mechanisms (see Goodner and Quatrano, 1993; Feijó et al., 1995). These mechanisms are undoubtedly complex and involve the regulation of numerous genes (Schiefelbein et al., 1993; Bouget et al., 1996; Lin et al., 1996). Pollen tube reorientation can occur in several minutes, and this might preclude a mechanism involving changes in gene expression. But mutants have been described in which pollen tubes are unable to locate the ovule, seemingly as a result of altered interactions with the stigma (Hülskamp et al., 1995). These mutants may then simply be unable to sense appropriate directional cues in the stigma and ovary.

In pollen tubes, the existence of a tip-focused gradient of cytosolic free calcium ($[Ca^{2+}]_c$) has been shown to be essential for growth (Obermeyer and Weisenseel, 1991; Rathore et al., 1991; Miller et al., 1992; Malhó et al., 1994; Pierson et al., 1994); it is maintained by an asymmetric activity of Ca^{2+} channels (Malhó et al., 1995). When *Agapanthus umbellatus* pollen tubes were impaled with a microelectrode and subjected to brief ionophoresis, immediate increases in $[Ca^{2+}]_c$ in the vicinity of the microinjection were observed (Malhó et al., 1994). Pollen tube growth ceased but recovered with a new growth axis and in an orientation up to ±90° from the original direction. These observations could be mimicked by photolysis of loaded caged Ca^{2+} (nitr-5). The tip-focused $[Ca^{2+}]_c$ gradient could be detected as re-forming before the recovery of growth, and the distribution of the gradient seemed to predict the new growth orientation (Malhó et al., 1995); this observation was later confirmed by Pierson et al. (1996). When pollen tubes

[1] To whom correspondence should be addressed.

were subjected to weak reorienting electrical fields, growth continued and the tip-focused gradient was maintained, but increases in $[Ca^{2+}]_c$ throughout the pollen tube cytoplasm were again also observed (Malhó et al., 1994, 1995). Including very low concentrations of the tip Ca^{2+} channel blocker lanthanum in the medium did not inhibit growth but did inhibit electrical field–dependent reorientation (Malhó et al., 1994, 1995).

We believe that the implication of the above-mentioned data is that there might be at least two separate ways in which $[Ca^{2+}]_c$ could manipulate growth orientation—one involving the body of the tube (perhaps through modification of the microfilament structure) and the other involving manipulation of the Ca^{2+} gradient at the tip. To distinguish between these possibilities and to identify the spatial position of the motor(s) that is responsible for orientation/reorientation, we examined the response of different pollen tube cytoplasmic domains to localized Ca^{2+} changes. There are at least two ways in which these Ca^{2+} changes can be achieved. The first involves loading a UV-sensitive caged Ca^{2+} or a UV-sensitive caged Ca^{2+} chelator into the pollen tube and achieving spatially restricted release by using a xenon arc/flash photolysis system (Zucker, 1995) and a controllable aperture that confines the spread of the UV beam. The second consists of externally supplying ionophores and channel blockers asymmetrically to the tip of the tube by using a microelectrode. We combined both of these systems with confocal microscopy to permit immediate imaging of the response. We found that localized increases of $[Ca^{2+}]_c$ within the apical dome of the pollen tube modify and control growth direction.

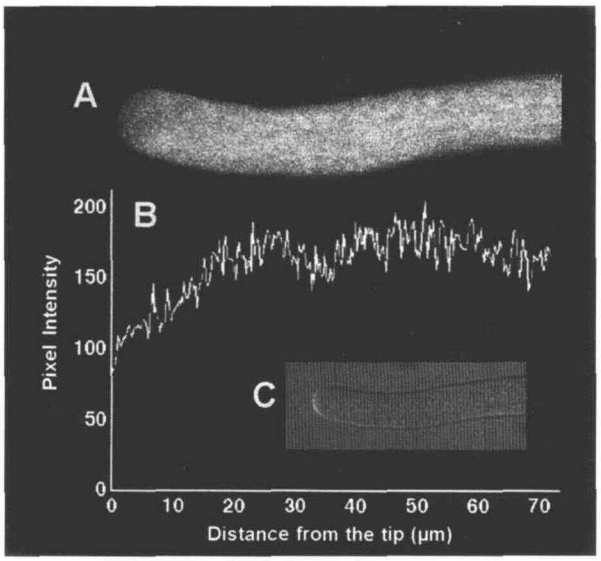

Figure 1. Distribution of Loaded Calcium Green-1 in a Growing *A. umbellatus* Pollen Tube, Using Confocal Microscopy.

The fluorescent dye was loaded by ionophoresis and imaged after 15 min (recovery time, 1 to 5 min).

(A) and **(B)** The fluorescent image and the distribution of pixel intensity along a midline transect down the length of the apical 70 μm, respectively.

(C) The transmitted light image (reduced to approximately half size) collected concomitantly with the fluorescent image to certify that the imaging is being performed in a median section of the tube.

RESULTS

Confocal Imaging of $[Ca^{2+}]_c$ with Calcium Green-1

Use of the ratio dyes fura-2 and indo-1 attached to dextrans has distinct long-term advantages for imaging Ca^{2+} gradients in pollen tubes (Pierson et al., 1994). However, because these dyes require UV excitation, they are unsuitable for experiments involving the release of UV photoactivable caged probes. Imaging before release would be precluded because UV excitation for $[Ca^{2+}]_c$ measurement would result in continued caged probe photolysis. In this case, the less satisfactory method of single wavelength dyes must be used. Calcium Green-1 was the dye of choice because of its high quantum yield. We have established four criteria that we and others (Pierson et al., 1994) believe must be met before Calcium Green-1 is used in these experiments.

First, the dye must be evenly distributed in the cytoplasm and of sufficient pixel strength throughout the experimental period (normally <15 min) to permit observations of $[Ca^{2+}]_c$ changes. Figure 1A shows a confocal image of a growing pollen tube loaded with Calcium Green-1. The distribution of the dye is fairly homogenous, with the exception of the tip clear zone where the signal is more reduced (Figure 1B), even though we are observing an optically thin plane through the pollen tube. This finding suggests that Calcium Green-1 is excluded from this region. Even so, we found that pixel intensity in this area provided a signal strong enough for reliable quantification. To minimize errors due to change in cell shape, we excluded the first 0.5 μm of the cell perimeter from all measurements. Any pollen tube with an average pixel intensity in the apical dome that was >50 (for an eight-byte image) was considered potentially artifactual and was discarded. As before, we were unable to detect the tip-based Ca^{2+} gradient using Calcium Green-1 and the confocal microscope but could readily detect the gradient using fluorescence ratio imaging with indo-1 (Malhó et al., 1994). One possibility is that this difference might result from the real depth of the Ca^{2+} gradient directly beneath the plasma membrane, but this question clearly needs further investigation.

Second, it remains to be determined whether fluorescence loss or dye leakage is perturbing $[Ca^{2+}]_c$ measurements. In a previous report (Malhó et al., 1994), we showed that fluorescence loss due to bleaching and/or dye leakage was not significant through the longest incubation period used here (<15 min) and did not perturb measurements.

Third, images must be maintained in the midplane of the pollen tube. The optical arrangement used for this study has an axial resolution of ~2 μm, so it is important to collect images in the midplane of the cell (Read et al., 1992; Pierson et al., 1996). Pollen tubes sometimes change their growth direction within the z-axis; therefore, we used the second detector on our confocal microscope to collect a transmitted light image (Figure 1C). With this procedure, we ensured that the signal collected was coming from the midsection of the tube, thus reducing potential artifacts due to a change in path length.

Fourth, the dye must be stable in the cytoplasm. A potential problem with using an unattached single wavelength dye is the sequestration of dyes into organelles. We found no evident sequestration within the window of time necessary for our experiments (see Figure 1A), but it begins to be visible in older regions of the tube 20 min after loading.

Resolution of the Imaging and Photoactivating System

The area of irradiation by the focused UV beam was determined both in vitro and in vivo by using caged fluorescein, which is only weakly fluorescent until the fluorescein is released. For in vitro measurements, caged fluorescein was incorporated into agar. After UV flash photolysis, the fluorescent area was imaged in the confocal microscope and measured. In vivo measurements were made by loading caged fluorescein into growing pollen tubes and again imaging the fluorescence after UV photolysis. We found, with both in vitro and in vivo studies, that we could confine photoactivation to circular areas of ~80 to 95 μm^2 (~10 to 11 μm in diameter). Figure 2 shows the results of instantaneous photolysis of caged fluorescein inside a pollen tube and its subsequent rapid diffusion, presumably accelerated by streaming, throughout the cell.

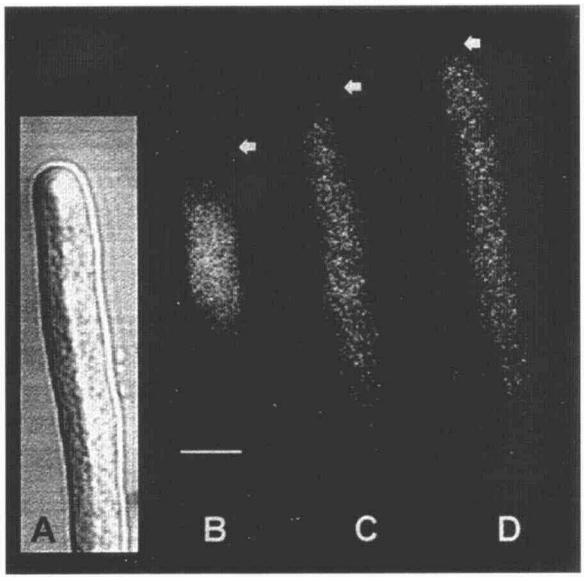

Figure 2. Distribution of Fluorescein after Localized UV Photolysis of Loaded Caged Fluorescein in a Growing *A. umbellatus* Pollen Tube.

Caged fluorescein was loaded by ionophoresis.
(A) Transmitted light image before photoactivation.
(B) to **(D)** The distribution of released fluorescein was imaged by using confocal microsocopy at 5, 20, and 40 sec, respectively, after flash photolysis through a controlled aperture. **(B)** indicates the length of the UV beam at the point of impact on the pollen tube. The arrows indicate the tip of the pollen tube. Bar in **(B)** = 10 μm for **(B)** to **(D)**.

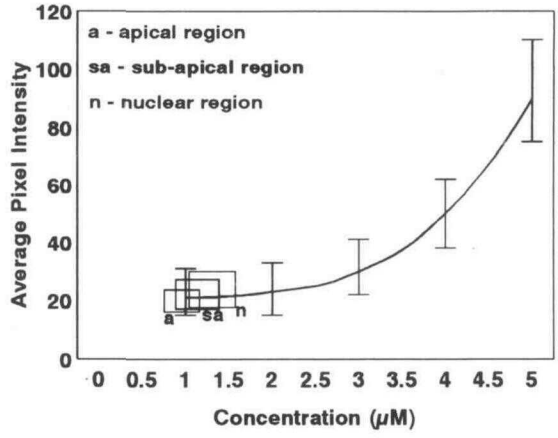

Figure 3. UV Photolysis of Caged Fluorescein and Calibration of Released Fluorescein in Different Regions of a Growing *A. umbellatus* Pollen Tube.

Pollen tubes were loaded with caged fluorescein, and localized photolysis was performed in the nuclear (n), subapical (sa), and apical (a) regions. Confocal microscopy was used to determine the fluorescence intensity emitted by the different regions. Molarities of fluorescein released were determined by comparision with a calibration curve constructed in vitro with 8- to 12-μm-diameter water droplets in oil solution containing known amounts of fluorescein. Boxes indicate signal variation in different regions of the pollen tubes (n = 15).

Because the pollen tube is thinner at the tip, we quantified the apparent efficacy of caged fluorescein photolysis in different parts of the pollen tube by comparing the fluorescence emitted by the cells with that of water droplets with known concentrations of fluorescein (Figure 3). As with dye distribution, there is a slight gradient of apparent cage photolysis efficacy further away from the tip. However, the amount of fluorescent light released from the lowest caged fluorescein concentrations is too close to the limit of detection to make a more accurate calibration. We can expect a similar pattern for apparent photolysis efficiency distribution of other caged molecules; however, exact quantitation is more difficult, because the photolysis quantum efficiency in many cases is not known and the extent of prior accumulations of caged molecules in the tip may be different for the different molecules. Figure 2 also indicates that the cage itself is probably nontoxic

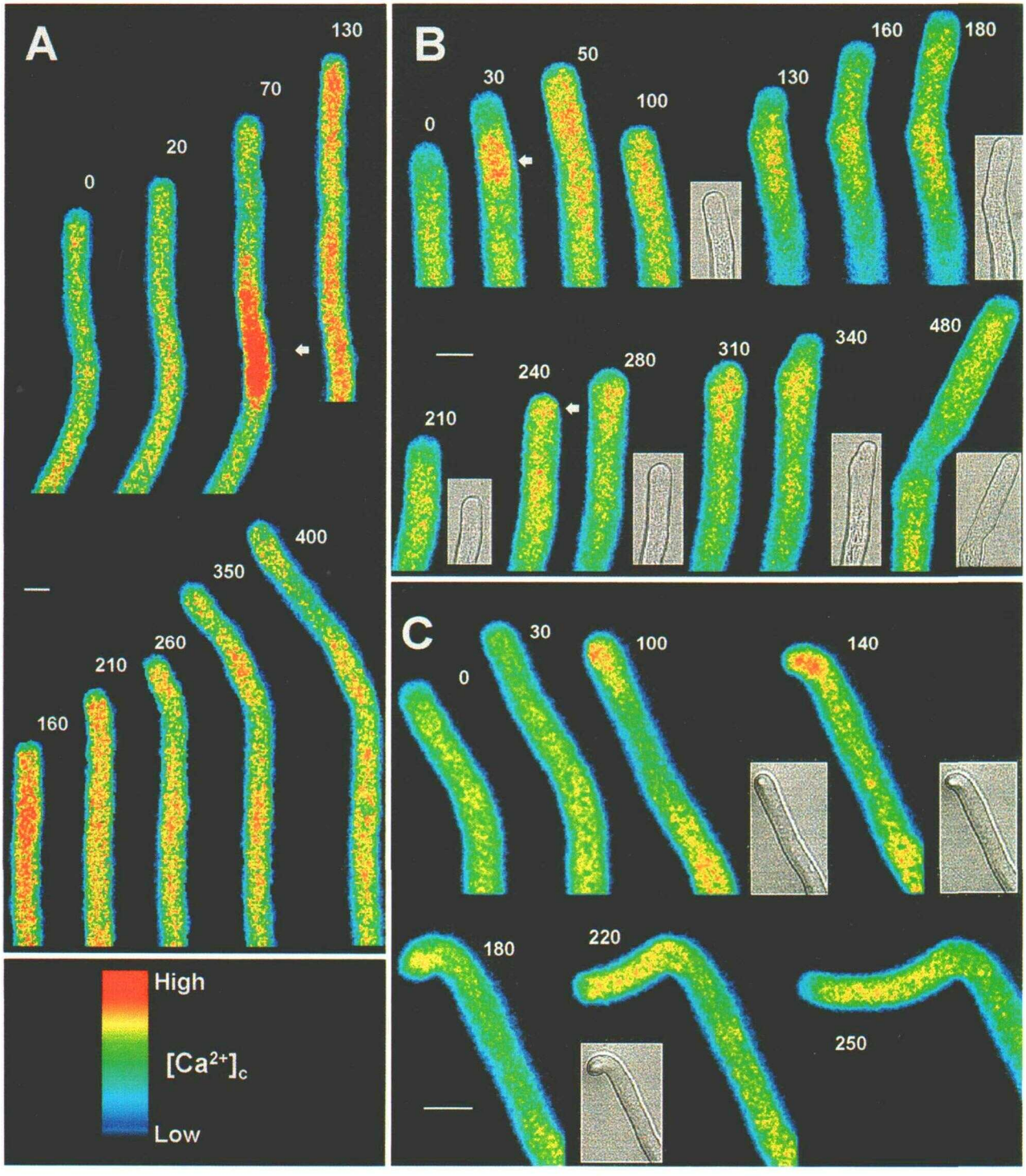

Figure 4. Effect of UV Photolysis of Loaded Nitr-5 in Different Regions of a Growing *A. umbellatus* Pollen Tube on the Distribution of $[Ca^{2+}]_c$ and Orientation.

(A) Confocal time-course series of images in which nitr-5 was flash photolyzed in the nuclear zone (arrow) at ~65 sec. The times (sec) at which images were taken are shown adjacent to the tip of the growing tube. Random reorientation of the pollen tube growth axis occurs after the elevation in $[Ca^{2+}]_c$ reaches the tip; this occurs ~60 sec after photoactivation. The images are displayed with the color coding explained below. Bar = 10 μm.

because the pollen tube continues normal rates of growth after release.

According to Zucker (1995), use of this system allows photolysis release rates of 80 to 90% in one flash if a high numerical aperture (NA) and good UV transmission objective are used. With the objective used in this study, we found that the maximal release of caged fluorescein is achieved only after the third pulse, with ~60% release with the first pulse. We have routinely used only one light pulse because fast pulse repetition could not be achieved with this system. We also decided not to compromise further the optical quality for image acquisition and chose not to use the quartz objectives normally employed for UV light (see Methods).

Effect of Localized Photoactivation of Nitr-5 on Pollen Tube $[Ca^{2+}]_c$ and Orientation

Photoactivation of nitr-5 (and later diazo-2) was performed in different regions of the pollen tube: the nuclear region, 30 to 50 μm behind the tip; the subapical region, 15 to 30 μm behind the tip; and the apical dome, 0 to 15 μm from the tip. Imaging data is found in Figure 4, and quantification of these data is found in Figure 5. With the single wavelength dye Calcium Green-1, we cannot directly compare fluorescence levels from different parts of the tube to determine absolute $[Ca^{2+}]_c$. However, the magnitude of the changes in fluorescence (similar to the ratio of maximum to minimum fluorescence, F_{max}/F_{min} for single wavelength dyes; Williams et al., 1993) is directly proportional to the changes in the levels of $[Ca^{2+}]_c$ (Haugland, 1993). With this approach and our previous absolute estimates of $[Ca^{2+}]_c$ in *A. umbellatus* using indo-1 (Malhó et al., 1994, 1995), we found that the increase in $[Ca^{2+}]_c$ resulting from nitr-5 photolysis in the nuclear region is substantially higher than that which occurs in the subapical and apical regions (400 to 700 nM compared with 300 to 500 nM). These increases are similar to those we have determined before for nitr-5 photolysis in guard cells and protoplasts (Gilroy et al., 1990; Shacklock et al., 1992; Allan et al., 1994). Absolute calibration of $[Ca^{2+}]_c$ in cells, however, is recognized as very difficult, using either single or ratio dyes, so these numbers should be regarded only as estimates.

When the nitr-5 photolysis was performed in the nuclear region (n = 7; five tubes showing reorientation), an immediate increase in $[Ca^{2+}]_c$ was observed in this area (Figure 4A). In the following second, this elevation spreads toward other regions at a variable speed of 65 to 75 μm min^{-1} (Figures 4A and 5A). When the elevation reached the tip, pollen tubes either showed just a transient decrease in growth rates or were temporarily arrested. Upon recovery, a reorientation of the growth axis was recorded in most cells. In agreement with our previous report (Malhó et al., 1994), the subsequent growth orientation induced by release in the nuclear region is random within ±90° of the original direction. We have observed similar responses when caged inositol 1,4,5-trisphosphate was released in *A. umbellatus* pollen tubes (Malhó, 1995).

When photolysis of nitr-5 was performed in the subapical region (Figure 4B, 30 sec), the $[Ca^{2+}]_c$ elevation usually resulted in a transient but complete arrest of tube growth (n = 10; eight pollen tubes exhibited reorientation). The pollen tubes recovered (~1 min later), and the reorientation of the growth axis was evident but again was random. Some pollen tubes responded with only a decrease in growth rates, but even most of these reoriented. Similar results were obtained when Ca^{2+} was released in the overall apical region (Figure 4B, 240 sec). In six cells, growth was arrested, and when they recovered (~1 min later), the direction of growth had clearly altered. In another four pollen tubes, apical bursting was observed. Therefore, we investigated another six cells with a reduced concentration of nitr-5 in the loading microelectrode (0.5 mM), but only two of these showed subsequent curvature. This finding suggests that a threshold concentration of $[Ca^{2+}]_c$ must be exceeded for curvature to be initiated.

In our previous study (Malhó et al., 1995), we commented that the $[Ca^{2+}]_c$ gradient appeared to re-form on the side on which growth would subsequently appear (see Pierson et al., 1996). We decided therefore to draw a midline through the apical dome and determine the ratio of the fluorescence on the left side compared with that on the right (similar to F_{max}/F_{min}; Williams et al., 1993) (Figure 5, diagram). This ratio should then reflect the difference in $[Ca^{2+}]_c$ on both sides of the dome. If this ratio directed subsequent orientation, correlated curvature changes should become apparent. Therefore, we decided to mimic the variation in the ratio of fluorescence of the dome by photolysing nitr-5 only on the left-hand side. This was accomplished by focusing the UV beam on the edge

Figure 4. (continued).

(B) Confocal time-course series of images in which nitr-5 was flash photolyzed in the subapical zone at ~25 sec and in the apical zone at ~235 sec (arrows). The times (sec) at which images were taken are shown adjacent to the tip of the growing tube. Black and white images are the transmitted light images in register with the fluorescent ones showing the morphology of the tip (reduced to approximately half size). In both cases there was a change in pollen tube growth direction to the right side. Bar = 10 μm.

(C) Confocal time-course series of images in which nitr-5 was flash photolyzed in the left hemisphere of the apical zone at ~95 sec. The times (sec) at which images were taken are shown adjacent to the tip of the growing tube. Black and white images are the transmitted light images in register with the fluorescent ones showing the morphology of the tip (reduced to approximately half size). A pronounced reorientation of the pollen tube growth axis follows the localized elevation in $[Ca^{2+}]_c$ in the left side of the tube apex. Bar = 10 μm.

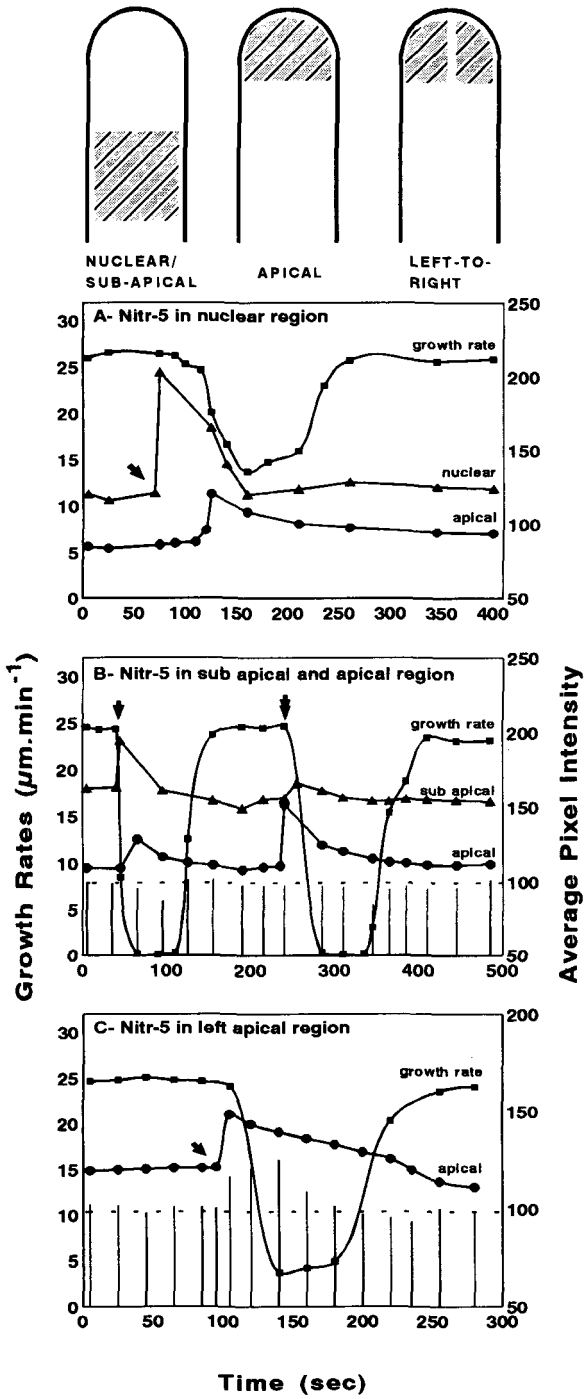

Figure 5. Quantitative Estimates of Data in Figure 4 (Growing *A. umbellatus* Pollen Tubes Loaded with Nitr-5).

Filled squares (■) represent growth rates. Calcium Green-1 pixel intensity in subapical or nuclear regions is represented by filled triangles (▲); in the apical region, pixel intensity is indicated by filled circles (●). Vertical bars represent the ratio of pixel intensities (expressed in percentages) between the left and the right hemisphere of the tube apex (~10 μm² each). The diagram above the graphs illustrates the area analyzed in each region of the pollen tube for pixel intensity measurements: the nuclear and subapical regions are 130 μm² (~29,000 pixels); the apical region is 95 μm² (~21,000 pixels); and the apical left or right region is 45 μm² (~10,000 pixels).

(A) Flash photolysis of loaded nitr-5 in the nuclear region. The data are estimated from the experiment shown in Figure 4A. Average pixel intensity of Calcium Green-1 was determined in the nuclear (▲) and the apical (●) regions. Note the delay between the release of Ca^{2+} in the nuclear region (arrow) and the increase in $[Ca^{2+}]_c$ in the apical region. The decrease in the growth rates, which occurs when $[Ca^{2+}]_c$ is elevated in the apex, is concomitant with the reorientation.

(B) Effect of photolysis of loaded Nitr-5 in the apical left-to-right ratio (vertical bars) and pixel intensity in the subapical (▲) and apical (●) regions. The data are estimated from Figure 4B. The left-to-right ratio is ~100, except when the tube changes its growth direction (at 100 and 350 sec). Arrows indicate times of photoactivation.

(C) Photolysis of loaded nitr-5 in the left hemisphere of the apical region. Data are estimated from Figure 4C. The left-to-right ratio of Calcium Green-1 increases significantly upon bending of the pollen tube. Photoactivation is at the arrow.

of the pollen tube apex (n = 6; five tubes showed curvature to the left; in the remaining tube, growth was stopped with no curvature on recovery). Figures 4C and 5C show the results of one such experiment. After photoactivation, there was a localized increase in $[Ca^{2+}]_c$ that slowly declined after the release; $[Ca^{2+}]_c$ returned to resting levels when the cell resumed its normal growth. In this experiment, pollen tube growth was not totally arrested, and yet the highest angle of bending was recorded. Another interesting feature of this experiment was that the highest deviation to the ratio left to right occurred not immediately after photoactivation but when the cell started to bend (Figure 5C). This suggests that the release triggered a mechanism that kept $[Ca^{2+}]_c$ elevated in that region, leading in turn to cell bending.

We found that indeed the direction of the growth axis could be predicted in every experiment in which nitr-5 was photolyzed (n = 41). When the ratio value was plotted (as a percentage), it was found that values above 100, before growth recovery, resulted in reorientation to the left, and values below 100 resulted in reorientation to the right. The highest angles of reorientation resulted in the highest deviation in the ratio value from 100 (Figure 6; median angle of reorientation of 29°).

Effect of Localized Photoactivation of Diazo-2 on Pollen Tube $[Ca^{2+}]_c$ and Orientation

To determine whether a decrease in $[Ca^{2+}]_c$ might control orientation, we loaded the pollen tubes with diazo-2, a caged Ca^{2+} chelator. Photoactivation of diazo-2 in the nuclear or

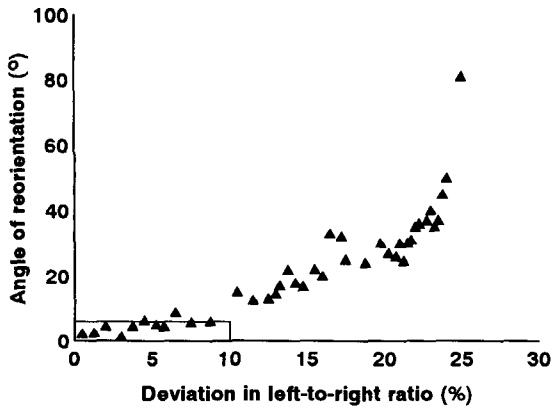

Figure 6. Correlation Plot of Orientation Angle versus Deviation in Left-to-Right Ratio in 41 Cells in Which Nitr-5 Was Photolyzed in Different Growth Regions.

The points inside the boxed region represent the cells in which the angle of reorientation and/or the deviation in the left-to-right ratio was considered nonsignificant and was excluded from the calculation of the median angle of reorientation.

subapical region (n = 10; six tubes showed curvature; data not shown) resulted in a decrease of $[Ca^{2+}]_c$ and a transient inhibition of pollen tube growth. This effect is similar to the reports of 1,2-*bis*(*o*-aminophenoxylethane *N,N,N',N'*-tetraacetic acid (BAPTA) injection into pollen tubes (Miller et al., 1992). Photoactivation of loaded diazo-2 directly in the apical region (n = 7; only two tubes recovered) often resulted in tip bursting, suggesting that certain minimal values of $[Ca^{2+}]_c$ are important for apical integrity. Furthermore, pixel intensity was often reduced to levels that we consider to be below the confidence limit and thus were not suitable for imaging. Reduction of diazo-2 concentration in the loading needle only partly solved these problems; however, even in the best cases, pollen tubes that survived the photoactivation possessed an abnormal morphology. Figure 7A shows one of these tubes. A release of diazo-2 in the left side of the apical region (n = 7; only four recovered) led to a strong reduction of the growth rates and some bending toward the opposite side (Figure 7A, 90 sec). However, tip growth was disturbed, as can be seen in Figure 7A (180 to 350 sec). Bending was also preceded by a reduction in the apical left-to-right ratio (Figure 8A).

Modification of Internal Apical $[Ca^{2+}]_c$ by External A23187 and $GdCl_3$

The data shown above suggest that reorientation can be induced by localized increases in $[Ca^{2+}]_c$ in the apical region. To further assess the validity of this hypothesis, we needed to induce asymmetric distributions of apical $[Ca^{2+}]_c$ by alternative means. Consequently, we loaded A23187 and $GdCl_3$ into microelectrodes and simply placed these near the tips of growing pollen tubes. We reasoned that the low rates of diffusion from the narrow orifice of the microelectrode might set up diffusion gradients across the tip and thus differentially interfere with the tip-focused $[Ca^{2+}]_c$ gradient. Imaging data are shown in Figures 7B and 7C, and Figures 8B and 8C show quantitative estimates from these. Although these sets of experiments could be achieved with dual-wavelength dyes, we decided not to do so, because the use of fura-2 or indo-1 implies the use of completely different equipment for fluorescence imaging with characteristics of its own. Thus, any results could not be compared directly. Furthermore, Pierson et al. (1996) showed that Ca^{2+} values in the tip of the pollen tube may be underestimated because fura-2 is saturated in that region and thus no longer allows extremely accurate measurements. Calcium Green-1 has a lower affinity for Ca^{2+}, which allows us to perform measurements at higher concentrations.

When the pollen tubes were exposed to a gradient of A23187 across the tip, eight of 10 pollen tubes responded positively to the stimulus, showing bending toward the ionophore source and an increase in $[Ca^{2+}]_c$ that was most evident in the side closer to the electrode (Figure 7B). The bending was also accompanied by a decrease in growth rate and in the apical left-to-right ratio (Figure 8B). Once the microelectrode was removed, which was essential if growth was to continue, further curvature ceased and straight growth was resumed. Growth rates then returned to normal with an apical left-to-right ratio close to 100%. The remaining two cells showed no visible response.

Exposure to $GdCl_3$ from a microelectrode, on the other hand (Figure 7C), induced bending away from the microelectrode in seven of 10 pollen tubes. The remaining three tubes exhibited total growth inhibition after the treatment. The curvature was accompanied by a decrease in growth rate and increase in the apical left-to-right ratio (Figure 8C). The overall fluorescence from the apical zone showed a slight reduction, suggesting a reduction in apical $[Ca^{2+}]_c$.

Undulating Pollen Tubes Show Oscillations in $[Ca^{2+}]_c$ between the Left- and Right-Hand Sides of the Dome

It is a common observation that many pollen tubes growing in vitro exhibit slight wiggling from side to side. It is generally assumed that these wiggles reflect the lack of appropriate guidance cues. However, some of our in vitro–grown pollen tubes (<1%) showed repetitive and unusually high angles of bending (e.g., Figure 9). This enabled us to test the hypothesis that even without external stimulation, a change in growth axis is preceded by changes in apical $[Ca^{2+}]_c$, particularly the apical left-to-right ratio. When $[Ca^{2+}]_c$ was measured in these tubes (Figure 10A), we observed that the left-to-right ratio oscillated following the general pattern of wiggling (Figure 10B). We also found that whenever the cell bent, there was a reduction in growth rate. The accuracy and time interval of our

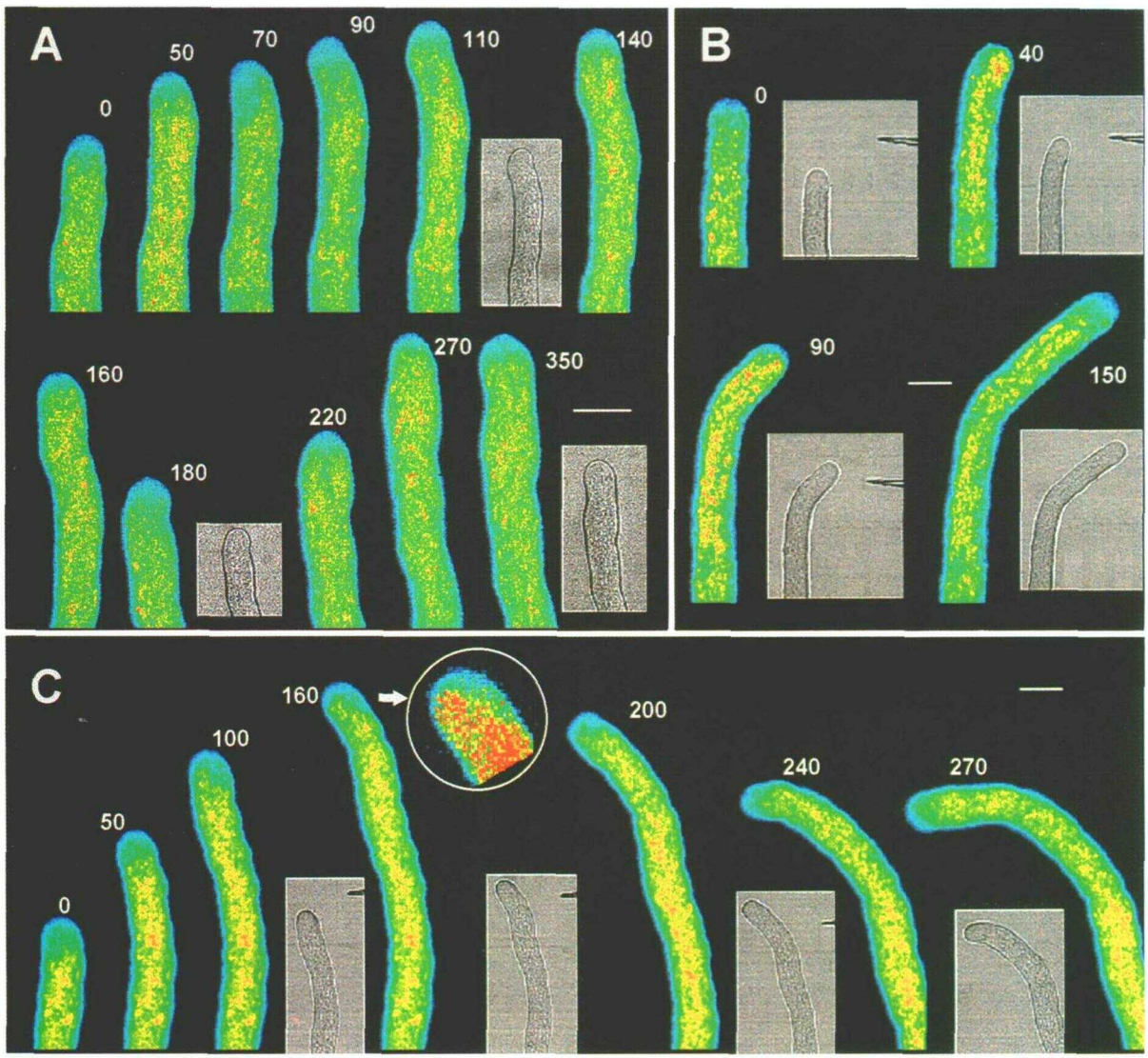

Figure 7. Effect of UV Photolysis of Loaded Diazo-2 or Exposure to External Gradients of A23187 or $GdCl_3$ on $[Ca^{2+}]_c$ and Orientation in a Growing *A. umbellatus* Pollen Tube.

(A) Confocal time-course series of images in which diazo-2 was flash photolyzed in the left hemisphere of the apical zone at ~65 sec. The times (sec) at which images were taken are shown adjacent to the tip of the growing tube. Black and white images are the transmitted light images in register with the fluorescent ones showing the morphology of the tip (reduced to approximately half size). After photoactivation, there was a reorientation of the pollen tube growth axis but also a perturbation of the tip growth mechanism evident in the morphology of the apical region. The color images are displayed with the coding shown in Figure 4. Bar = 10 μm.

(B) Confocal time-course series of images taken after placement of a microelectrode containing A23187 near to the tip of a pollen tube. The times (sec) at which images were taken are shown adjacent to the tip of the growing tube. Black and white images are the transmitted light images in register with the fluorescent ones showing the morphology of the tip (reduced to approximately half size). The ionophore is diffusing from a microelectrode that was removed at ~95 sec to prevent toxic effects. The tube bends toward the ionophore source. The color images are displayed with the coding shown in Figure 4. Bar = 10 μm.

(C) Confocal time-course series of images taken after placement of a microelectrode containing $GdCl_3$ near to the tip of a pollen tube. The times (sec) at which images were taken are shown adjacent to the tip of the growing tube. Black and white images are the transmitted light images in register with the fluorescent ones showing the morphology of the tip (reduced to approximately half size). The circled image is a magnification of the tip shown next. The inhibitor is diffusing from the microelectrode that was removed at ~215 sec. The tube bends away from the channel blocker. The color images are displayed with the coding shown in Figure 4, except for the circled image in which color was intensified to enhance differences. Bar = 10 μm.

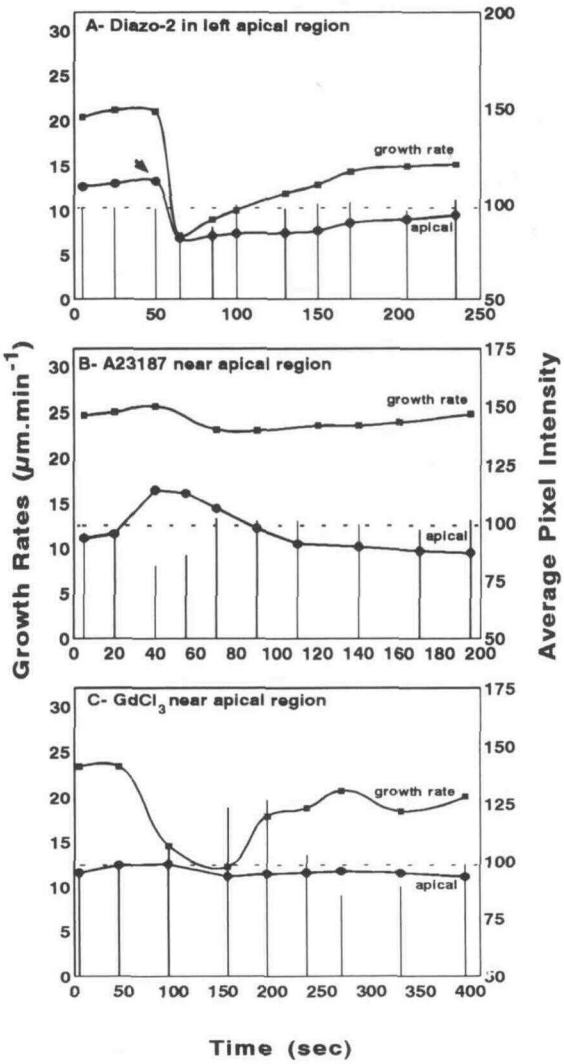

Figure 8. Quantitative Estimates of Data in Figure 7 (Growing *A. umbellatus* Pollen Tubes Loaded with Diazo-2 or Exposed to External Gradients of A23187 or $GdCl_3$).

Filled squares (■) represent growth rates. Calcium Green-1 pixel intensity in the apical region is represented by filled circles (●). Vertical bars represent the ratio of pixel intensities (expressed in percentages) between the left and right hemispheres of the tube apex (~10 μm^2 each). The areas analyzed are explained in the diagram of Figure 5.

(A) Photolysis of diazo-2 in the left apical hemisphere. Data are estimated from Figure 7A. Upon photoactivation (arrow) in the left apical region, the left-to-right ratio of the hemisphere shows a substantial decrease; however, this was not followed by a marked reorientation but instead by a perturbation in tip growth.

(B) Effects of placing a microelectrode containing A23187 near the tip of a growing pollen tube. Data are estimated from the experiment shown in Figure 7B. The ratio decrease is accompanied by bending toward the ionophore source.

(C) Effects of placing a microelectrode containing $GdCl_3$ near the tip of a growing pollen tube. Data are estimated from the experiment shown in Figure 7C. Bending away from the microelectrode is accompanied by an increase in the left-to-right ratio.

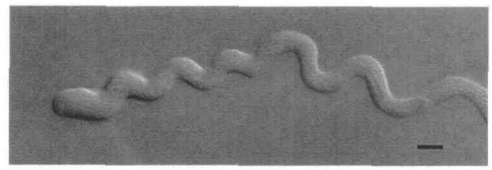

Figure 9. Differential Interference Contrast Microscopy of an Undulating Pollen Tube.

Bar = 10 μm.

imaging system were not sufficient to provide a detailed growth rate curve under these conditions; nevertheless, it too also seemed to be oscillatory. In the majority of pollen tubes showing more limited wiggling, the changes in apical fluorescence were too low to be considered significant (<10%).

DISCUSSION

Analysis of the Imaging System

Ca^{2+} imaging in living plant cells is a very powerful technique to unravel the mechanisms of signal perception and transduction. However, special care needs to be taken because of the many potential artifacts that have been described and referred to earlier (Read et al., 1992; Fricker et al., 1993). Although the use of a single-wavelength dye precludes accurate quantitation, it does not prevent assessment of differences that result from signaling. In many cases, it is this information that is most crucial. Pierson et al. (1996) pointed out the importance of using ratiometric procedures in all studies in which optical pathlength is an issue, such as in pollen tubes, and we concur with this statement; unfortunately, it is not always possible to use ratiometric dyes. Ratiometric Ca^{2+} dyes need UV light for excitation, so whenever caged probes are to be used, one must choose a single-wavelength dye.

Fluo-3, probably the most popular of these dyes, was designed specifically for use with photolabile chelators (Kao et al., 1989), and several techniques to achieve calibrations have been described (Williams et al., 1993). In apical growing cells, which are highly differentiated, none of these techniques is beyond criticism; still, the use of single-wavelength dyes in the past has proven to be very useful in detecting qualitative changes in $[Ca^{2+}]_c$ (Gilroy et al., 1990; Shacklock et al., 1992; Read et al., 1993). Calcium Green-1 has one very advantageous feature: it has a high-quantum yield, allowing imaging to be performed with up to 50 times lower intracellular concentrations, thus reducing any putative buffering effect on $[Ca^{2+}]_c$. Recently, a new ratioable indicator using visible light for excitation has become available. However, the indicator consists of two conjugated dyes (Texas Red and Calcium Green-1), and its usefulness still needs to be assessed properly in light of differential photobleaching rates of the two fluorophores. Furthermore, this dye is available only in the 70-kD dextran

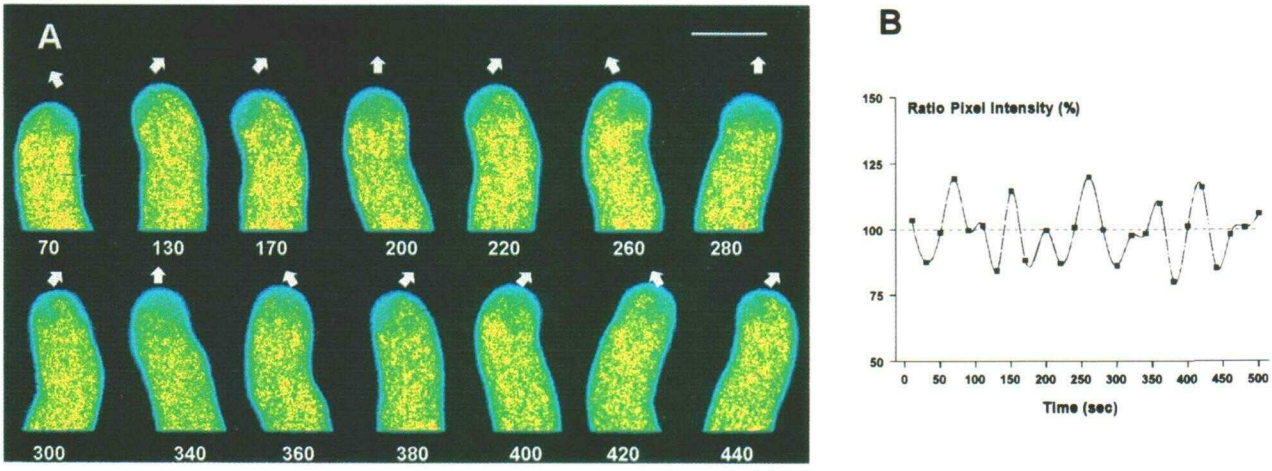

Figure 10. Estimates of the Left-to-Right Ratio of Pixel Intensity and Growth of a Vigorously Undulating Pollen Tube.

Confocal microscopy of loaded Calcium Green-1 fluorescence was performed, and the left-to-right hemisphere ratios of the apical zone were calculated. The images are displayed with the color coding shown in Figure 4.

(A) Tips of the same growing pollen tube at the times (sec) indicated at the base. See corresponding left-to-right ratio value in **(B)**. The arrows indicate the future direction of the tip. Bar = 10 μm.

(B) Time course of the fluorescence ratio (percentage) between the left and right hemispheres of the tube apex. Whenever the tube bends to the left, the ratio increases to >100; when the ratio is below that value, the tube grows to the right. An oscillatory pattern is clear.

form. Despite the several advantages of dextran dyes (Haugland, 1993; Pierson et al., 1996), their introduction into the cell requires pressure microinjection, making the recovery of small cells such as *A. umbellatus* pollen tubes more difficult.

Among the advantages of dextrans are their reduced cytotoxicity and stability in the cytoplasm. We have found that when a "mild" ionophoresis is performed, these criteria also apply to Calcium Green-1 free acid, at least during the time of our experiments (usually ~10 min). In previous studies (Malhó et al., 1994, 1995) and in this one, we show that cytotoxicity is not a problem in *A. umbellatus*. Sequestration of Calcium Green-1 into organelles does not become obvious within the first 20 min, except in older regions of the tube that were not analyzed in this study. By using confocal microscopy and fast-scan modes, we reduce photobleaching to a minimum while reducing problems due to path length by collecting thin optical sections. In addition, we used the second detector on our confocal to collect a transmitted light image and to certify that the image collected was in the midplane of the cell apex.

Ca^{2+} Signaling in Pollen Tubes

The results obtained in this work show new and interesting aspects of Ca^{2+} signaling in pollen tubes. It is clear that the sensitivity of tip growth to transient increases in $[Ca^{2+}]_c$ depends on the cytological zones of the cell in which calcium is elevated. For instance, the photoactivation of nitr-5 in the nuclear region resulted in higher releases of Ca^{2+}, presumably because the concentration of the caged molecule was higher in this area (although other reasons, e.g., vesicle density, cannot be excluded). Based on the increase in fluorescence recorded immediately after photolysis, we estimated that the amount of Ca^{2+} released was 400 to 700 nM in the nuclear region and 300 to 500 nM in the apical region. However, the effects on pollen tube orientation were much more significant when Ca^{2+} was released in the apex, because in this case, direct effects on subsequent curvature were observed. In addition, when the loading concentration of nitr-5 was reduced, there was a significant increase in the number of pollen tubes showing no response. This result suggests that a certain threshold in $[Ca^{2+}]_c$ must be reached before a cellular response is triggered.

A similar interpretation can be made from the experiments with nuclear release. When Ca^{2+} was released in this region, a signal of high $[Ca^{2+}]_c$ spread wave-like toward the other regions of the cell. The response was triggered only when the signal reached the tip. In half of the cells, growth was arrested totally, whereas in the other half, only a transient reduction in growth rates was recorded. Again, evidence for the existence of threshold values is present, but it is difficult to be precise because our imaging does not allow an accurate measurement of absolute $[Ca^{2+}]_c$.

The spreading wave–like character of the high $[Ca^{2+}]_c$ signal also has interesting features: it may involve a Ca^{2+}-induced, Ca^{2+} release mechanism, and the speed of travel is approximately similar to a slow Ca^{2+} wave (Jaffe, 1993). Ca^{2+}-induced Ca^{2+} release has the characteristics of an au-

tocatalytic process, meaning that due to positive feedback, a small Ca^{2+} release will be amplified until the release process is terminated by negative feedback. Recent experiments with poppy pollen tubes suggest that inositol phosphates could also be involved in this wave-like movement of $[Ca^{2+}]_c$ because these pollen tubes contain a Ca^{2+}-activated phospholipase C (Franklin-Tong et al., 1996), and it is possible to envisage a relay mechanism involving both the release of Ca^{2+} and the activation of the phospholipase C. In *A. umbellatus* pollen tubes, there seems to be some attenuation when the signal moves from the nuclear to the apical region, but smooth grading of Ca^{2+} release in intact cells is known to occur by the progressive recruitment of independent elementary units, such as Ca^{2+} puffs and sparks, that individually contribute a quantized amount of Ca^{2+} (Bootman and Berridge, 1995). This attenuation might explain why release in the apical region has more drastic effects (e.g., bursting) than in the nuclear region.

The diffusion pattern of Ca^{2+} was quite different from that of the released fluorescein. Ca^{2+} has a low mobility in the cytosol; it binds to numerous proteins, it is sequestered by organelles, and it is released from intracellular stores and pumped out and into the cell. The propagation of a Ca^{2+} wave is therefore an extremely complex process involving different cellular compartments. In contrast, the diffusion of fluorescein most likely results from a translocation in bulk by rapid streaming.

Reducing $[Ca^{2+}]_c$ levels by release of diazo-2 did not have the opposite effect to increasing them. When release of diazo-2 was achieved in the nuclear or subapical region, the results were fairly similar to the equivalent experiment with nitr-5. This agrees with the observations of pollen tube arrest by injection of BAPTA buffers (Miller et al., 1992; Pierson et al., 1994). Indeed, any mild treatment that dissipates the tip-focused $[Ca^{2+}]_c$ gradient can result in the destruction of the previous polar axis and the regeneration of a new one. The extent of reorientation probably depends not only on the treatment but also on the pollen used. For instance, in lily pollen tubes, treatment with caffeine, which transiently inhibits growth, resulted in almost no reorientation (Pierson et al., 1996). But when diazo-2 was released in the *A. umbellatus* apical zone, the pollen tubes either burst or showed subsequent abnormal growth, suggesting that a perturbation of tip elongation had also occurred. This is unlikely to be a side reaction resulting from the release of the caging molecule because no such effect was observed when release was performed further back from the tip. The cytoplasmic streaming in pollen tubes would rapidly distribute such molecules, as we showed with photolysis of caged fluorescein (Figure 2). The sudden decrease in $[Ca^{2+}]_c$ from diazo-2 release probably interferes with more than just the ionic balance. Otherwise, similar effects would be expected when the channel blocker Gd^{3+} was applied via a microelectrode in the extracellular medium. The pollen tube elements that may be affected by diazo-2 photolysis are phospholipid binding annexins (Blackbourn et al., 1992; Battey and Blackbourn, 1993), extensins (Rubinstein et al., 1995), deposition of wall material (Li et al., 1994), or cytoskeletal elements (Kohno and Shimmen, 1987). Thus, it seems likely that pollen tubes respond more effectively to an increase in $[Ca^{2+}]_c$ than to a decrease.

Apical $[Ca^{2+}]_c$ Controls Growth Direction—The Role of Ca^{2+} Channels

The localized photorelease of Ca^{2+} within the apical region changed the direction of pollen tube growth. These observations confirm our previous data (Malhó et al., 1994, 1995) and strongly support the suggestion by Pierson et al. (1996) that the location of the highest $[Ca^{2+}]_c$ domain within the tip defines the point from which elongation will proceed. In a straight-growing pollen tube, the highest $[Ca^{2+}]_c$ domain is represented by a Ca^{2+} hotspot located underneath the plasma membrane at the midpoint of the apical dome (the apical midpoint). Inducing pollen tube reorientation by photolysis of nitr-5 in one side of the apical region clearly indicates that the distribution of $[Ca^{2+}]_c$ within the apical dome is not only a consequence of tip growth but also plays an important role in determining the growth direction.

The presence of the tip-focused $[Ca^{2+}]_c$ gradient is associated with a cluster of active Ca^{2+} channels (Malhó et al., 1995). Because control of orientation is crucial to the arrival of the pollen tube at the micropyle, the control of active Ca^{2+} channels becomes central to the mechanisms that ensure successful fertilization. Our experiments with ionophores and inhibitors show that by asymmetrically promoting or inhibiting Ca^{2+} influx (thus mimicking asymmetrically modified Ca^{2+} channel activity), we are able to modify tube direction. Ding and Pickard (1993) recently suggested that Ca^{2+} channels, activated by stretching of the plasma membrane, respond to a variety of external stimuli and act as sensors of cell turgor, external mechanical stresses, and chemical gradients. Stretch-activated Ca^{2+} channels are likely to be present in pollen tubes, as suggested by our work with Gd^{3+}, an inhibitor of stretch-activated ion channels (Yang and Sachs, 1989), and by the effect of increased osmolarity in reducing the $[Ca^{2+}]_c$ gradient (Pierson et al., 1994). Stretch-activated channels are also voltage dependent (Guharay and Sachs, 1985), and we have shown that pollen tubes respond to external electrical fields with a membrane depolarization and localized Ca^{2+} influx (Malhó et al., 1995). Direct evidence for the existence of voltage-dependent Ca^{2+} channels that are activated by depolarization of the plasma membrane of higher plant cells has been obtained by Huang et al. (1994) and Thuleau et al. (1994a, 1994b).

Our previous work with Mn^{2+} quenching of indo-1 (Malhó et al., 1995) suggests that Ca^{2+} channels are located all over the apical dome, but as suggested by Pierson et al. (1996), they must be particularly active (or dominant) in the extreme apex, the apical midpoint. It has long been recognized that to maintain the structure of the dome, there must be a gradient of growth from the center outward. This implies a gradient in the tension applied to the plasma membrane and thus a

gradient in open stretch-activated channels. Asymmetrically changing this gradient should alter the influx of Ca^{2+} in specific domains of the dome, modifying in turn vesicle fusion, cytoskeletal structure, and pollen tube growth direction (Hepler et al., 1994; Pierson et al., 1994; Feijó et al., 1995).

The hypothesis that the gradient of Ca^{2+} channel activity is determined by the position of the apical midpoint itself is certainly supported by our data on photoactivation of loaded nitr-5 on the left side of the apical region. In these experiments, we observe that although $[Ca^{2+}]_c$ starts to decrease immediately after photorelease, the left-to-right fluorescence ratio continues to increase until complete growth reorientation is achieved (Figure 5C). This suggests that the apical midpoint of Ca^{2+} channel activity can be moved to new positions by changes in $[Ca^{2+}]_c$ itself. It further suggests that the distribution of channels and $[Ca^{2+}]_c$ is in some way homeostatically regulated, even when Ca^{2+} influx is initially asymmetric. We suggest that these homeostatic mechanisms are intimately coupled to the positioning of the apical midpoint. The fact that the angle of reorientation does not exceed a certain value (>90°) also suggests the existence of negative feedback controls leading to the closure of previously open channels and vice versa. We believe that the distribution of open and closed channels in the apical plasma membrane is therefore in a constant dynamic state. In turn, the position of the apical midpoint is probably subject to continuous assessment and realignment.

The existence of control mechanisms that specify the spatial distribution of open and closed channels can help to explain aspects of the extreme undulating pattern of the small number of pollen tubes that we described in Figure 9. We assume that the wiggling associated with the growth of these tubes results from a longer than usual delay in the negative feedback mechanism determining the distribution of open and closed channels. In these cases, the result is a constant slow oscillation of the apical midpoint, the hotspot, around the hemisphere of the dome. Such oscillations can easily be initiated by any slight external perturbation or even by a stochastic opening of more channels on one side of the dome than on another.

We observed that these pollen tubes can cease the extreme undulations after a period of time and assume a more normal growth pattern. Of possible relevance to this discussion is the finding that high concentrations of Mn^{2+} in the growth medium (2 mM), which can enter Ca^{2+} channels, result in a 10-fold increase of pollen tubes showing this growth pattern (R. Malhó and A. Moutinho, unpublished data). Release of Ca^{2+} from intracellular stores may also play a part in this mechanism. Lancelle and Hepler (1992) demonstrated the presence of endoplasmic reticulum profiles in the apical region that could act as a source of intracellular Ca^{2+}, and the results in this study agree with the existence of a possible Ca^{2+}-induced Ca^{2+}-release mechanism. Early experiments using chlorotetracycline demonstrated a gradient of membrane-associated Ca^{2+} (Reiss and Herth, 1978), but these studies must be reanalyzed with more advanced techniques, such as organelle targeting of aequorin (Rizzuto et al., 1993; Johnson et al., 1995).

Ca^{2+} channels are unlikely to be the only regulators of tip growth direction. K^+ channels have also been suggested to be involved in this mechanism (Obermeyer and Kolb, 1993; Feijó et al., 1995), and our studies with inhibitors cannot rule out the possibility that different channels are also being affected. Unfortunately, the distribution and role of other ions in tip growth are virtually unknown. Gradients of H^+ were not detected in growing pollen tubes (R. Parton, S. Fischer, R. Malhó, T. Jelitto, and N.D. Read, submitted manuscript), and maintenance of an intracellular pH seems to be important for cell viability rather than tip growth.

Pollen Tube Guidance—A Possible Role for Extracellular Ca^{2+}?

The guidance mechanisms of pollen tube growth in vivo are subject to considerable debate, and the role of extracellular Ca^{2+} in pollen tube reorientation is probably one of the most controversial issues. Plant cells are known to respond to changes in extracellular Ca^{2+} (Bush, 1995; McAinsh et al., 1995), and regions of high Ca^{2+} have been described along the path of the pollen tube from the stigma to the ovule (Chaubal and Reger, 1990). However, our study failed to show that pollen tubes are attracted to these regions because of Ca^{2+} itself. Mascarenhas and Machlis (1962) showed that in vitro, pollen tubes grew from regions of very low Ca^{2+} toward regions of higher Ca^{2+}; however, when pollen was grown in a medium with 1 mM Ca^{2+}, the tubes no longer showed a response to higher concentrations. The same authors showed that chemotropism toward ovules was overcome by the addition of Ca^{2+} to the growth medium. We observed similar results when Ca^{2+} was allowed to diffuse from a microelectrode placed on one side of the tip; in a Ca^{2+}-rich medium, the tubes did not bend toward higher Ca^{2+} (R. Malhó and A. Moutinho, unpublished data). Recently, the first reports of a chemotropic molecule have been published (Cheung et al., 1995; Wu et al., 1995) that show the isolation of a floral transmitting tissue-specific glycoprotein. There is also strong evidence that hydroxyproline-rich proteins may facilitate the adhesion of pollen to the stigma surface and the growth of tubes along the style (Sanders and Lord, 1992; Gane et al., 1995). It is interesting to speculate that some of these proteins may interact with the tube plasma membrane, creating localized tension that could then activate Ca^{2+} channels. Alternatively, pollen tubes may have an extracellular Ca^{2+}-sensing receptor as described for animal cells (Brown et al., 1995). Because gravitropic bending is thought to be regulated by extracellular Ca^{2+} concentrations in the root cap exudate (Björkman and Cleland, 1991; Baluska et al., 1996), the search for this particular protein in plants would be relevant without studies of pollen tubes themselves.

METHODS

Plant Material

Pollen of *Agapanthus umbellatus* was harvested and stored, and pollen tubes were grown in vitro, as described previously (Malhó et al., 1994). Composition of the culture medium was modified to achieve higher growth rates and thus reduce the time necessary for each experiment: 2.5% sucrose, 0.01% H_3BO_3, 0.02% $MgCl_2$, 0.02% $CaCl_2$, and 0.02% KCl, pH 6.0, at 27°C.

Imaging and Calibration of $[Ca^{2+}]_c$

Growing pollen tubes were microinjected with the free acid of the Ca^{2+}-sensitive dye Calcium Green-1 (Molecular Probes Inc., Eugene, OR). The cells were ionophoresed with Calcium Green-1 (1 mM) for 1 to 2 min at 0.1 to 0.2 nA and allowed to recover fully before experimental treatment. Details of the experimental procedure and criteria used to establish the success of microinjection can be found in Malhó et al. (1994). Only pollen tubes that recovered with no deviation from the focal plane were chosen for later analysis.

Cystolic free calcium ($[Ca^{2+}]_c$) was imaged by means of laser scanning confocal microscopy using an MRC-600 (Bio-Rad Microscience Ltd., Hemel Hempstead, UK) equipped with a 25-mW argon laser (Read et al., 1992) and enhanced photomultiplier tubes. A 3% laser intensity was used to excite Calcium Green-1 at 488 nm while collecting simultaneously a transmitted light image through a fiber optic. All images were collected in the F2 mode (0.75 sec per frame) using a Nikon 60× plan apo objective (numerical aperature [NA] = 0.95) (Nikon UK Ltd., Telford, UK). Higher NA objectives could not be used due to their shorter working distance. For fluorescence imaging, the black level and the gain settings were adjusted in each experiment to allow an average background pixel intensity of between 0 and 10 and a fluorescent signal coming from the pollen tube of between 60 and 220. Pollen tubes showing lower signals or dye saturation under these imaging conditions were discarded. The detector aperture was kept constant for an optical section of ~2.0 to 2.5 μm in depth; such depth of field results in an uneven voxel value in the tip of the pollen tube, but it was necessary to collect a signal strong enough to be analyzed (R. Parton, S. Fischer, R. Malhó, T. Jelitto, and N.D. Read, submitted manuscript). For bright-field imaging, a gain setting of 3.0 and a black level of 5.0 were used; the detector aperture was identical to the fluorescence imaging. A zoom factor of 3.0 was used except for experiments with photoactivation of caged biomolecules in the nuclear region of the pollen tubes where the zoom was reduced to 2.0. The time interval between image acquisition was 10 sec, except when adjustments had to be made on the field of view for repositioning the tube tip. Fluorescence was quantified in terms of average pixel intensity by using the histogram command of COMOS/MPL software (Bio-Rad). Only changes >10% were considered significant for our data.

Loading and Photoactivation of Caged Biomolecules

$[Ca^{2+}]_c$ values were artificially manipulated by photoactivating caged Ca^{2+} (nitr-5) and a caged Ca^{2+} chelator (diazo-2). Nitr-5 (0.5 to 1 mM) (Calbiochem, Nottingham, UK) and diazo-2 (0.1 to 0.5 mM) (Molecular Probes) were microinjected together with Calcium Green-1 (same ionophoretic conditions). Photoactivation was performed by exposing the pollen tubes to an ~1-msec pulse of UV light (300 mJ in the 330- to 380-nm band) from a XF-10 flash photolysis system (Hi-Tech Scientific, Salisbury, UK) equipped with a xenon arc lamp (Rapp and Guth, 1988). The area of photoactivation was controlled by means of an iris diaphragm placed between the UV lamp and the objective.

To assess the system efficiency and resolution (both temporal and spatial), the pollen tubes were loaded by ionophoresis with 3000 kD of dextran anionic caged fluorescein (Molecular Probes) (1 to 2 mM in the needle). The fluorescence emitted after photoactivation was compared with the fluorescence resulting from photoactivation of in vitro solutions: water droplets with a diameter of 8 to 12 μm and known concentrations of caged fluorescein (1 to 10 μM) were dispersed in a mineral oil solution and used as an approximate indicator for the in vivo concentration of the caged biomolecules (Allan et al., 1994). However, despite similar net charge, nitr-5 and diazo-2 have different molecular weights, so similar ionophoretic conditions may result in slightly different concentrations of these two caged molecules.

Effect of External Gradients

$[Ca^{2+}]_c$ was also imaged in pollen tubes loaded with Calcium Green-1 and exposed to external gradients of the ionophore A23187 or the Ca^{2+} channel $GdCl_3$ (Sigma-Aldrich Co., Dorset, UK). The gradients were imposed by diffusion of stock solutions (100 μM A23187 or $GdCl_3$ made in growth medium) from a pressure microelectrode (external diameter, ~1 to 2 μm) placed near the tip of the growing tubes.

Conventional Light Microscopy

Whenever needed, pollen tubes were examined with a Nikon Microphot FX-A by using differential interference contrast optics and a 40× oil objective (1.4 NA). Light micrographs were recorded on Kodak 400 TMAX 35-mm film rated at 800 ASA.

Growth Reorientation and Numerical Data Presentation

Reorientation of pollen tubes was defined as a change in the growth axis of >5°, either to the left or right (Malhó et al., 1994).

Numerical data presented correspond to single-cell analysis of typical experiments and not to summary statistics. This is because there is a certain degree of variability on not only the biological level but also the technical one. Even minor changes in the degree of loading, amount of photolyzed biomolecule, area of release (or diffusion from microelectrode), disturbance on microinjection, and responsiveness of the cell can all play a role in the extent of cellular response.

ACKNOWLEDGMENTS

We thank Salomé Pais and Dr. Nick Read for their support and critical suggestions, Richard Parton for the great discussions on confocal scanning laser microscopy, and Dr. Andrew Allan for his help with the photolysis system. R.M. acknowledges the European Union for a short-term fellowship (Project of Technical Priority grant). The work was supported by the Biotechnological and Biological Science Research

Council (Swindon, UK) and Junta Nacional de Investigação Científica e Tecnológica (Lisbon, Portugal) (Grant No. PBICT/P/BIA/2068/95).

Received May 13, 1996; accepted July 30, 1996.

REFERENCES

Allan, A.C., Fricker, M.D., Ward, J.L., Beale, M.H., and Trewavas, A.J. (1994). Two transduction pathways mediate rapid effects of abscisic acid in *Commelina* guard cells. Plant Cell **6,** 1319–1328.

Baluska, F., Volkmann, D., Hauskrecht, M., and Barlow, P.W. (1996). Root cap mucilage and extracellular calcium as modulators of cellular growth in postmitotic growth zones of the maize root apex. Bot. Acta **109,** 25–34.

Battey, N.H., and Blackbourn, H.D. (1993). The control of exocytosis in plant cells. New Phytol. **125,** 307–338.

Björkman, T., and Cleland, R.E. (1991). The role of extracellular free-calcium gradients in gravitropic signaling in maize roots. Planta **185,** 379–384.

Blackbourn, H.D., Barker, P.J., Huskisson, N.S, and Battey, N.H. (1992). Properties and partial protein sequence of plant annexins. Plant Physiol. **99,** 864–871.

Bootman, M.D., and Berridge, M.J. (1995). The elemental principles of calcium signaling. Cell **83,** 675–678.

Bouget, F.-Y., Gerttula, S., Shaw, S.L., and Quatrano, R.S. (1996). Localization of actin mRNA during the establishment of cell polarity and early cell divisions in *Fucus* embryos. Plant Cell **8,** 189–201.

Brown, E.M., Vassilev, P.M., and Hebert, S.C. (1995). Calcium ions as extracellular messengers. Cell **83,** 679–682.

Bush, D.S. (1995). Calcium regulation in plant cells and its role in signaling. Annu. Rev. Plant Physiol. Plant Mol. Biol. **46,** 95–122.

Chaubal, R., and Reger, B.J. (1990). Relatively high calcium is localized in synergid cells of wheat ovaries. Sex. Plant Reprod. **3,** 98–102.

Cheung, A.Y., Wang, H., and Wu, H.-m. (1995). A floral transmitting tissue-specific glycoprotein attracts pollen tubes and stimulates their growth. Cell **82,** 383–393.

Ding, J.P., and Pickard, B.G. (1993). Mechanosensory calcium-selective cation channels in epidermal cells. Plant J. **3,** 83–110.

Feijó, J.A., Malhó, R., and Obermeyer, G. (1995). Electrical currents, ion channels and ion pumps during germination and growth of pollen tubes. Protoplasma **187,** 155–167.

Franklin-Tong, V.E., Drøbak, B.K., Allan, A.C., Watkins, P.A.C., and Trewavas, A.J. (1996). Growth of pollen tubes of *Papaver rhoeas* is regulated by a slow-moving calcium wave propagated by inositol 1,4,5-trisphosphate. Plant Cell **8,** 1305–1321.

Fricker, M., Tester, M., and Gilroy, S. (1993). Fluorescence and luminescence techniques to probe ion activities in living plant cells. In Fluorescent and Luminescent Probes for Biological Activity, W.T. Mason, ed (London: Academic Press), pp. 360–377.

Gane, A.M., Clarke, A.E., and Bacic, A. (1995). Localization and expression of arabinogalactan proteins in the ovaries of *Nicotiana alata* Link and Otto. Sex. Plant Reprod. **8,** 278–282.

Gilroy, S., Read, N.D., and Trewavas, A.J. (1990). Elevation of cytoplasmic calcium by caged calcium or caged inositol trisphosphate initiates stomatal closure. Nature **346,** 769–771.

Goodner, B., and Quatrano, R.S. (1993). *Fucus* embryogenesis: A model to study the establishment of polarity. Plant Cell **5,** 1471–1481.

Guharay, F., and Sachs, F. (1985). Mechanotransducer ion channels in chick skeletal muscle: The effects of extracellular pH. J. Physiol. **363,** 119–134.

Haugland, R. (1993). Intracellular ion indicators. In Fluorescent and Luminescent Probes for Biological Activity, W.T. Mason, ed (London: Academic Press), pp. 34–43.

Hepler, P.K., Miller, D.D., Pierson, E.S., and Callaham, D.A. (1994). Calcium and pollen tube growth. In Pollen–Pistil Interactions and Pollen Tube Growth, A.G. Stephenson and T.-h. Kao, eds (Rockville, MD: American Society of Plant Physiologists), pp. 111–123.

Heslop-Harrison, J. (1987). Pollen germination and pollen tube growth. Int. Rev. Cytol. **107,** 1–78.

Huang, J.W., Grunes, D.L., and Kochian, L.V. (1994). Voltage-dependent Ca^{2+} influx into right-side-out plasma membrane vesicles isolated from wheat roots: Characterization of a putative Ca^{2+} channel. Proc. Natl. Acad. Sci. USA **91,** 3473–3477.

Hülskamp, M., Schneitz, K., and Pruitt, R.E. (1995). Genetic evidence for a long-range activity that directs pollen tube guidance in Arabidopsis. Plant Cell **7,** 57–64.

Jaffe, L.F. (1993). Classes and mechanisms of calcium waves. Cell Calcium **14,** 736–745.

Johnson, C.H., Knight, M.R., Kondo, T., Masson, P., Sedbrook, J., Haley, A., and Trewavas, A.J. (1995). Circadian oscillations of cytosolic and chloroplastic free calcium in plants. Science **269,** 1863–1865.

Kao, J.P.Y., Harootunian, A.T., and Tsien, R.Y. (1989). Photochemically generated cytosolic calcium pulses and their detection by fluo-3. J. Biol. Chem. **264,** 8179–8184.

Kohno, T., and Shimmen, T. (1987). Ca^{2+}-induced fragmentation of actin filaments in pollen tubes. Protoplasma **141,** 177–179.

Lancelle, S.A., and Hepler, P.K. (1992). Ultrastructure of freeze-substituted pollen tubes of *Lilium longiflorum*. Protoplasma **167,** 215–230.

Li, Y.Q., Chen, F., Linskens, H.F., and Cresti, M. (1994). Distribution of unesterified and esterified pectins in cell walls of pollen tubes of flowering plants. Sex. Plant Reprod. **7,** 145–152.

Lin, Y., Wang, Y., Zhu, J.-k., and Yang, Z. (1996). Localization of a Rho GTPase implies a role in tip growth and movement of the generative cell in pollen tubes. Plant Cell **8,** 293–303.

Malhó, R. (1995). Study of Pollen Grain Germination: Factors with Influence on Pollen Tube Elongation and Oriented Growth. PhD Dissertation (Lisbon, Portugal: University of Lisbon).

Malhó, R., Feijó, J.A., and Pais, M.S. (1992). Effect of electrical fields and external ionic currents on pollen tube orientation. Sex. Plant Reprod. **5,** 57–63.

Malhó, R., Read, N.D., Pais, M.S., and Trewavas, A.J. (1994). Role of cytosolic free calcium in the reorientation of pollen tube growth. Plant J. **5,** 331–341.

Malhó, R., Read, N.D., Trewavas, A.J., and Pais, M.S. (1995). Calcium channel activity during pollen tube growth and reorientation. Plant Cell **7,** 1173–1184.

Mascarenhas, J.P., and Machlis, L. (1962). Chemotropic response of the pollen of *Antirrhinum majus* to calcium. Plant Physiol. **39,** 70–77.

McAinsh, M.R., Webb, A.A.R., Taylor, J.E., and Hetherington, A.M. (1995). Stimulus-induced oscillations in guard cell cytosolic free calcium. Plant Cell **7,** 1207–1219.

Miller, D.B., Callaham, D.A., Gross, D.J., and Hepler, P.K. (1992). Free Ca^{2+} gradient in growing pollen tubes of *Lilium*. J. Cell Sci. **101,** 7–12.

Obermeyer, G., and Kolb, H.-A. (1993). K^+ channels in the plasma membrane of lily pollen protoplasts. Bot. Acta **106,** 26–31.

Obermeyer, G., and Weisenseel, M.H. (1991). Calcium channel blocker and calmodulin antagonists affect the gradient of free calcium ions in lily pollen tubes. Eur. J. Cell Biol. **56,** 319–327.

Pierson, E.S., Miller, D.D., Callaham, D.A., Shipley, A.M., Rivers, B.A., Cresti, M., and Hepler, P.K. (1994). Pollen tube growth is coupled to the extracellular calcium ion flux and the intracellular calcium gradient: Effect of BAPTA-type buffers and hypertonic media. Plant Cell **6,** 1815–1828.

Pierson, E.S., Miller, D.D., Callaham, D.A., van Aken, J., Hackett, G., and Hepler, P.K. (1996). Tip-localized calcium entry fluctuates during pollen tube growth. Dev. Biol. **174,** 160–173.

Rapp, G., and Guth, K. (1988). A low cost high intensity flash device for photolysis experiments. Pfluegers Arch. **411,** 200–203.

Rathore, K.S., Cork, R.J., and Robinson, K.R. (1991). A cytoplasmic gradient of Ca^{2+} is correlated with the growth of lily pollen tubes. Dev. Biol. **148,** 612–619.

Read, N.D., Allan, W.T.G., Knight, H., Knight, M.R., Malhó, R., Russell, A., Shacklock, P.S., and Trewavas, A.J. (1992). Imaging and measurement of cytosolic free calcium in plant and fungal cells. J. Microsc. **166,** 57–86.

Read, N.D., Shacklock, P.S., Knight, M.R., and Trewavas, A.J. (1993). Imaging calcium dynamics in living plant cells and tissues. Cell Biol. Int. **17,** 111–125.

Reiss, H.-D., and Herth, W. (1978). Visualization of the Ca^{2+}-gradient in growing pollen tubes of *Lilium longiflorum* with chlorotetracycline fluorescence. Protoplasma **97,** 373–377.

Rizzuto, R., Brini, M., Murgia, M., and Pozzan, T. (1993). Microdomains with high Ca^{2+} close to IP3-sensitive channels that are sensed by neighboring mitochondria. Science **262,** 744–747.

Rubinstein, A.L., Márquez, J., Suárez-Cervera, M., and Bedinger, P.A. (1995). Extensin-like glycoproteins in the maize pollen tube wall. Plant Cell **7,** 2211–2225.

Sanders, L.C., and Lord, E.M. (1992). A dynamic role for the stylar matrix in pollen tube extension. Int. Rev. Cytol. **140,** 297–318.

Schiefelbein, J., Galway, M., Masucci, J., and Ford, S. (1993). Pollen tube and root-hair tip growth is disrupted in a mutant of *Arabidopsis thaliana*. Plant Physiol. **103,** 979–985.

Shacklock, P.S., Read, N.D., and Trewavas, A.J. (1992). Cytosolic free calcium mediates red light-induced photomorphogenesis. Nature **358,** 753–755.

Thuleau, P., Moreau, M., Schroeder, J.I., and Ranjeva, R. (1994a). Recruitment of plasma membrane calcium-permeable channels in carrot cells. EMBO J. **13,** 5843–5847.

Thuleau, P., Ward, J.M., Ranjeva, R., and Schroeder, J.I. (1994b). Voltage-dependent calcium permeable channels in the plasma membrane of a higher plant cell. EMBO J. **13,** 2970–2975.

Williams, D.A., Cody, S.H., and Dubbin, P.N. (1993). Introducing and calibrating fluorescent probes in cells and organelles. In Fluorescent and Luminescent Probes for Biological Activity, W.T. Mason, ed (London: Academic Press), pp. 320–334.

Wu, H.-m., Wang, H., and Cheung, A.Y. (1995). A pollen tube growth stimulatory glycoprotein is deglycosylated by pollen tubes and displays a glycosylation gradient in the flower. Cell **82,** 395–403.

Yang, X.-C., and Sachs, F. (1989). Block of stretch-activated ion channels in *Xenopus* oocytes by gadolinium and calcium ions. Science **243,** 1068–1071.

Zucker, R. (1995). Photorelease techniques raising or lowering intracellular Ca^{2+}. In Methods in Cell Biology, Vol. 40, R. Nucitelli, ed (London: Academic Press), pp. 32–63.